FATIGUE CRACK GROWTH UNDER VARIABLE AMPLITUDE LOADING

Jihad A. SIDAWI
College of Engineering, CEEP
University of Bahrain
Issa Town, BAHRAIN

SUMMARY

Fatigue crack growth tests were conducted on an Fe 510 E C-Mn steel and a submerged arc welded joint from the same material under constant, variable, and random loading amplitudes. Paris-Erdogan's crack growth rate law was tested for the evaluation of m and C using the stress intensity factor K, the J-Integral, the effective stress intensity factor Keff, and the root mean square stress intensity factor Krms fracture mechanics concepts. The effect of retardation and residual stresses resulting from welding was also considered. It was found that all concepts gave good life predictions in all cases.

INTRODUCTION

Since most structural components are subjected in service to variable amplitude loading, a study of the fatigue behavior of the material under the effect of these loadings is essential. Different models contributed to a better understanding of the retardation or acceleration caused by the influence of load sequence (ref. 1-10). Further work is needed on the influence of these effects on fatigue lives.

Several authors have shown that residual stresses resulting from welding have a major influence on the fatigue lives of welded components (ref. 11-12). Modern sources studied this influence under the action of constant amplitude loading. Limited work on welded components subjected to variable amplitude loading have been deployed (ref. 13-14). This is due to the complexity of the problem under consideration.

The mechanism of failure under cyclic loading is a very complicated process. The fatigue strength of metals as well as welded joints is affected by a number of factors which determine fatigue life. The application of fracture mechanics showed that it is a suitable tool for the evaluation of fatigue lives not only for unwelded, but also for welded components (ref. 14-15)

In welded elements and components, cracks spend most of their lives growing (ref. 16). This fact is explained by the effect of inhomogeneities which usually exist in welded joints and which accelerates the initiation of cracks.

Irrespective of the mathematical expression of fatigue crack growth used, the expression must have the most essential parameters for solving the loading conditions as well as the material properties of a specific fatigue growth process (ref. 17). This fact is to be considered for both constant and variable amplitude loadings.

An estimation of the fatigue crack growth under variable amplitude loading can be done by assuming the existence of a threshold value ($\Delta K_o = 2$ MPa.m $^{1/2}$ for C and C-Mn steels) (ref. 18), and that the fatigue crack growth can be predicted by linear damage summation (ref. 19-20) such that the effect of load changes is ignored.

List of Symbols and Abbreviations

CCT: Center-Cracked-Tension test specimen or M(T): Middle - Tension.
CT : Compact-Tension test specimen.
ao [mm]: Initial crack length.
2a [mm]: Crack length of a CCT (MT) specimen 2a = 2x a (measured) + 2 ao.
a [mm]: Half crack length of a CT specimen a = a (measured) + ao.
N [kc]: Number of collapsed cycles.
da/dN [mm/kc]: Fatigue crack growth rate.
Fmin, Fmax, ΔF [kN]: Minimum, maximum loads and load range. (ΔF = Fmax-Fmin).
R : Load or stress ratio. Fmin/Fmax or Smin/Smax.
ΔK [MPa.m$^{1/2}$]: Stress intensity factor range.
ΔJel [N/m] : Elastic part of the cyclic J-integral range.
E [MPa] : Young's elastic modulus E= 2.06x 10^5 for C steels.
ΔJpl [N/m]: Plastic part of the cyclic J-integral range.
A [kN.mm] : Area under the force-displacement loop.
ΔJ [N/m] : Cyclic J-integral range.
ΔKeff [MPa.m$^{1/2}$]: Effective stress intensity factor range.
ΔKo [MPa.m$^{1/2}$]: Threshold value of the stress intensity factor range.
Reff : Effective load or stress ratio.
ΔS [MPa]: Stress range.
Re [MPa]: Yield strength (0.2Re).
ΔKrms [MPa.m$^{1/2}$]: Root mean square value of the stress intensity factor range.
m : Index in Paris-Erdogan's crack growth law da/dN = C $(\Delta K)^m$.
C : Coefficient in Paris-Erdogan's crack growth law.
Nt [kc]: Actual (tested) fatigue life {N(final)-N(initial)}.
Np [kc]: Predicted fatigue life: Np = $\int$ da/ C (ΔK)^m

Experimental Procedures

Test Materials

The material used in all experiments was from a 20mm thick C-Mn Fe 510 E steel plate. Weld joints were prepared by the submerged arc-welding technique, so that the weld line was perpendicular to the rolling direction of the material.

Chemical analysis and mechanical properties of Fe 510 E steel and weld metal are documented in table.1 and table.2 , respectively. Figure 1 shows the microstructure of the base metal and the weld metal. No trace of defects was observed in either the weld metal or the heat affected zone (HAZ), (width 3-4mm).

Welding Parameters and Technology:

A direct current ESAB welding machine was used with the positive pole on the electrode.

- Flux: N-70
- Filler wire: A-234 (Cast No.74035) (0.079%C- 1.14%Mn- 0.22%Si- 0.15%P- 0.018%S- 2.80%Ni (2%Ni spectral))
- Root run welding parameters: 400A- 30V- 35 m/h
- Beads: 450A- 32V- 35 m/h
- Preheating at 120° C
- Interpass temperature: 100-160° C (150° C).

Test Specimens

CCT (20x 120x 600 mm) and CT (20x 100 mm) specimens were machined from the plate. The direction of the loading axis was perpendicular to the weld line. The CCT notch was prepared by drilling a hole of ϕ4mm into the center of the polished pass in the middle of the width of the weld metal. Then, a thin sawcut was made on both sides of the hole such that the direction of the loading axis was kept perpendicular to the weld line. A sharp notched crack was made. The CT fatigue crack was oriented by a notch into the center of the weld metal.

Test Equipment and Machines

The CCT specimens were tested at room temperature at 5Hz in laboratory air using a 1600 KN servohydraulic Schenck fatigue testing machine connected to a computer. A cylindrical clip gauge was inserted into the ϕ4mm hole to measure the displacement range. The clip gage was also connected to the computer. From the computer two channels transferred the loading force and the displacement ranges

into a memory, from which the memorized cycle could be traced on a plotter. Another channel transferred the displacement range before entering into the memory to another plotter, which traced the crack opening displacement by time. From the first plotter both the loading forces and displacement ranges are then transferred into another computer programmed to integrate the area of the closed loop traced by the plotter and to calculate the loading force range and the displacement range as well.

The CT specimens were also tested by the same procedure using another Schenck fatigue testing machine at 40 Hz.

Identification of Specimens and Types of Loadings

The specimens can be identified by the material and type of loadings as follows:

1) BCA: Base metal constant amplitude loading ΔF_1
2) BVA: Base metal variable amplitude step low-high loading. $\Delta F_1 = 2\ \Delta F_2$
3) BRA: Base metal random amplitude loading.

To distinguish the weld metal from the base metal, a W replaced the B.

Table 1. Chemical Analysis of Fe 510 E Steel and Welded Metal SAW
[% Weight]

ANALYSIS	C	Mn	Si	P	S	Cr	Ni	Al	Nb
Base Metal	0.16	1.2	0.35	0.036	0.0216	0.05	0.03	0.04	0.02
Weld Metal	0.06	1.48	0.29	0.026	0.0172	0.11	2.23	0.01	0.00

Table 2. Mechanical Properties of Fe 510 E Steel and Weld Metal SAW

ANALYSIS	Yield Strength Re [MPa]	Tensile Strength Rm [MPa]	Elongation A [5%]	Contraction Z [%]	Toughness (20 °C) KCV [J.cm^{-2}]
Base Metal	430	572	27	57	108
Weld Metal	574	672	22	61	122

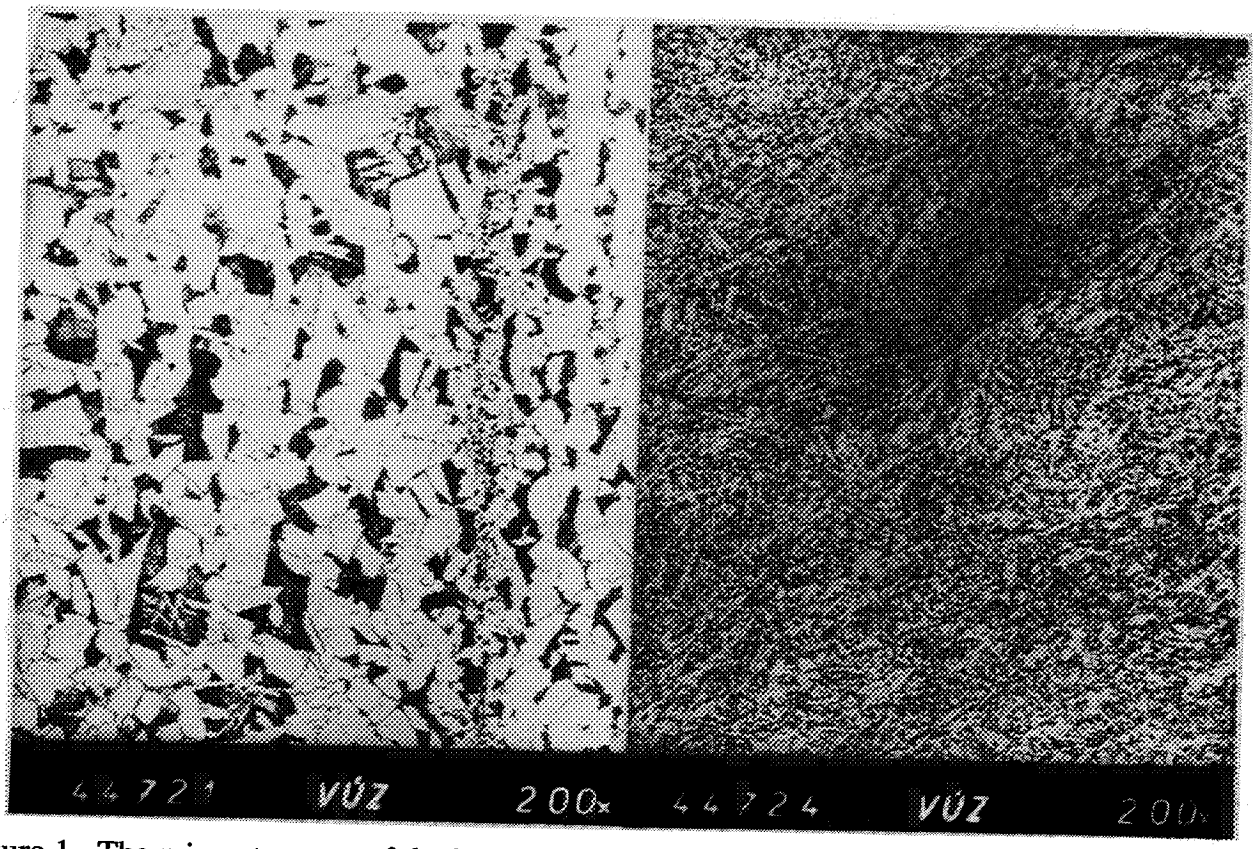

Figure 1. The microstructure of the base metal (left) and the weld metal (right) of Fe 510 E steel.

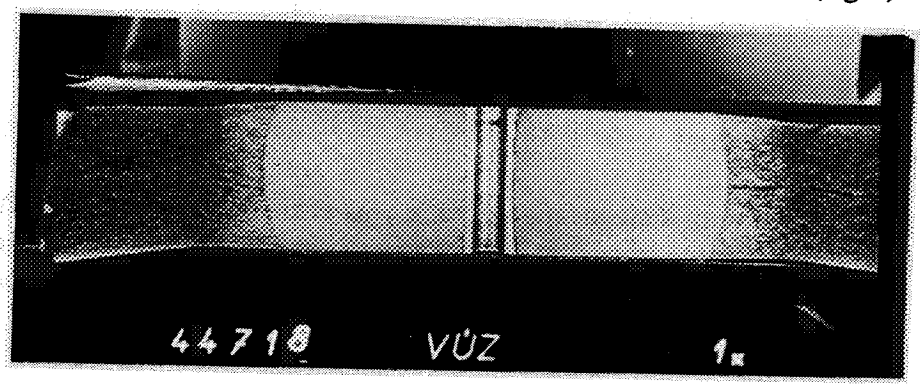

Figure 2. Fracture surface of a base metal, constant amplitude loading CCT specimen.

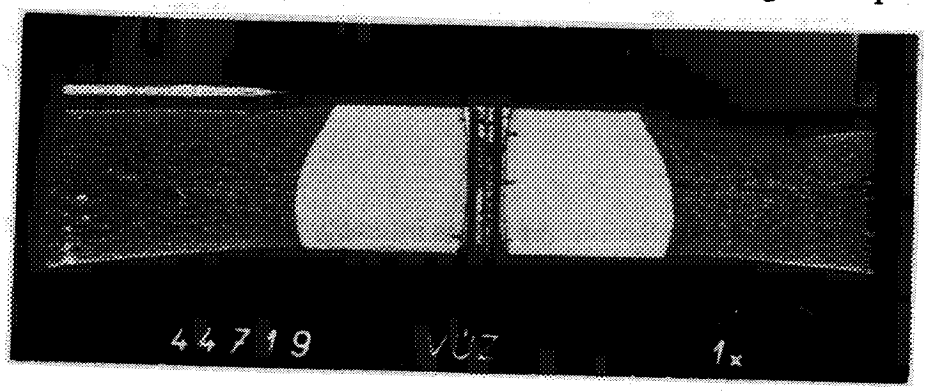

Figure 3. Fracture surface of a base metal, variable amplitude loading CCT specimen.

Fractographical Analysis

With the aid of a scanning electron microscope, fractographical analysis of the surface of the cracks was done. Four CCT specimens were analysed.

1) Base metal, constant amplitude loading. (Figure 2)
2) Base metal, variable amplitude loading. (Figure. 3)
3) Weld metal, constant amplitude loading.
4) Weld metal, variable amplitude loading.

The surface of the cracks in Figure 2 and Figure 3 can be relatively divided into a fine fracture surface and a coarse grained fracture surface, on which the rolled texture of the material is reflected.

While the specimen with a constant amplitude loading has a rubbering surface, without macroscopic traces, the one with variable amplitude loading has some narrow dark bands (striations). These are associated with the fact that the specimen was held at the mean load for some time until the replacing load was adjusted. These are sometimes called "Rest Bands". It is clear from the figures that the fatigue crack grew symmetrically around the central groove.

The only difference between the second series of specimens (Weld metal) and the first (Base metal) is that the inclusions in the weld metal are globular.

It is important to notice the fact that from the crack's micromorphological aspect, no difference between specimens subjected to constant or variable loading was observed.

Measured Data and Testing Procedure

All specimens were precycled until a clear fatigue crack was visually observed (min 2mm). The crack length was calculated from the average of two values measured visually by the aid of a scale attached to both the right and left side of the specimen. When possible four values were measured on both the front and back surfaces of the CCT specimen.

The loading forces were changed manually and checked by the computer readings. The displacement range and the area of the closed loop were also available on the computer readings. The mean displacement value was documented from the readings on the testing machine itself. It is important to note that the crack opening displacement measured is not the crack tip opening displacement.

Methods of Evaluation

Four methods were used for the prediction: the stress intensity factor, cyclic J-integral, effective stress intensity factor, and the root mean square stress intensity factor.

C and m were predicted using Paris-Erdogan's equation:

$$da/dN = C\,(\Delta K, \Delta J, \Delta Keff, \Delta Krms)^m \quad (1)$$

The ΔK for both the CCT and the CT types of specimens were calculated according to ASTM E 647-93 .The ΔJ values for CCT specimens were calculated using the Dowling (ref. 22) equations:

$$\Delta J = \Delta Jel + \Delta Jpl \quad (2)$$

$$\Delta Jel = \Delta K^2 / E \quad (3)$$

$$\Delta Jpl = A /[B (W-2a)] \quad (4)$$

The $\Delta Keff$ values were calculated using the recommendation of the IIW document (ref. 18), which suggested equations for $\Delta Keff$ prediction in air and sea water for 97.7% probability of survival. The Kopen was not experimentally measured.

Δ Keff :

a) Base metal (C-Mn steel):

$$\Delta K_o[N.mm^{-3/2}] = 170\text{-}214\ R \quad \text{for } 0 \le R \le 0.5 \quad (5)$$

or

$$\Delta K_o[\ MPa.m^{1/2}] = 5.375 - 6.767\ R \quad (6)$$

$$\Delta K_o = 63\ [N.mm^{-3/2}] \text{ or } \Delta K_o = 2\ [\ MPa.m^{1/2}] \quad \text{for } R \ge 0.5 \quad (7)$$

$$\Delta Keff = \Delta K \quad \text{for} \quad \Delta K > \Delta K_o/R \quad \text{and } R > 0 \quad (8)$$

$$\Delta Keff = (\Delta K - \Delta K_o)/(1- R) \quad \text{for } \Delta K \le \Delta K_o/R \quad (9)$$

b) Weld metal (C-Mn steel):

i) Constant amplitude loading:

$$\Delta K_o[N.mm^{-3/2}] = 214\ (\ \Delta S/Re)- 42 \quad (10)$$

or

$$\Delta K_o[\ MPa.m^{1/2}] = 6.767\ (\Delta S/Re)- 1.328 \quad (11)$$

$$\Delta K_o = 63\ [N.mm^{-3/2}] \text{ or } \Delta K_o = 2\ [\ MPa.m^{1/2}] \quad \text{if } \Delta S < Re/2 \quad (12)$$

$$\Delta S\ [MPa] = F/ (B.W) \quad (13)$$

Re [MPa]: 0.2% weld yield strength = 574 MPa.

$\Delta Keff = \Delta K$ for $\Delta K > \Delta K_0/Reff$ and $Reff > 0$ (14)

$\Delta Keff = (\Delta K - \Delta K_0)/(1 - Reff)$ for $\Delta K \leq \Delta K_0/Reff$ (15)

$Reff = (Re-\Delta S)/Re$ (16)

ii) Variable amplitude loading:

$\Delta K_0 = 63$ [$N.mm^{-3/2}$] or $\Delta K_0 = 2$ [$MPa.m^{1/2}$] (17)

The ΔKrms was calculated according to Barsom (ref. 23):

$$\Delta Krms = \sqrt{\sum_{i=1}^{k} (\Delta K_i)^2 / n} \quad (18)$$

where n= number of measurements.

Fatigue Crack Growth Results and Discussion

Fatigue crack growth results are presented in table 3. The most important features are discussed in what follows:

a) Addition of Small Loading Amplitudes.

The addition of small loading amplitude blocks to the constant amplitude block resulted in the decrease of the crack growth rates, thus in a significant increase in the fatigue lives as shown in table 3 (tested and predicted fatigue lives Nt and Np). This is also clearly illustrated in figures 4-6 in both cases, the base and the weld metals , and for the three types of evaluation methods K, Keff, and J-integral as well.

As half loading block amplitudes are added to the constant amplitude loading block, the fatigue lives were doubled (200%), while the growth rate showed a decrease by approximately the same amount as shown in figure 3 for specimens BVA and WVA. This has not been yet quantified by other authors, although the addition of small loads resulted in doubling the fatigue life. Figures 4-6 may indicate a family of parallel curves compared to the constant amplitude curves.

In the above shown figures 4-6, BRA and WRA specimens still show an improvement in fatigue lives of 1.5-4.0. This increase does not necessarily coincide with that of BVA and WVA. This is expected because of the randomness of the excess load applied.

Table 3. Fatigue Crack Growth Results of CCT Specimens

METHOD/ SPECIMEN		BCA	BVA	BRA	WCA	WVA	WRA
	Nt	26.8	72	110	37.9	70	55
K	m	3.586	3.149	2.847	2.496	1.969	1.947
	C	1.308^{-6}	3.589^{-6}	7.603^{-6}	3.464^{-5}	3.149^{-4}	3.903^{-4}
	Np	27.04	66.30	83.647	34.166	66.77	54.54
	Np/Nt	1.009	0.9209	0.7604	0.9789	0.9539	0.9916
J	m	1.7	1.451	1.379	1.197	0.963	0.968
	C	1.412^{-7}	6.775^{-7}	1.021^{-6}	7.124^{-6}	7.018^{-5}	8.369^{-5}
	Np	27.18	66.30	83.926	34.07	66.88	54.48
	Np/Nt	1.014	0.9209	0.7629	0.976	0.9555	0.9906
Keff	m	3.425	2.955	2.637	2.496	1.969	1.947
	C	2.524^{-6}	7.874^{-6}	1.696^{-5}	3.464^{-5}	3.149^{-4}	3.903^{-4}
	Np	27.09	66.93	84.039	34.166	66.77	54.54
	Np/Nt	1.011	0.9296	0.764	0.9789	0.9539	0.9916
Krms	m	-	3.149	1.964	-	1.969	3.182
	C	-	7.54^{-6}	3.592^{-4}	-	5.004^{-4}	4.78^{-6}
	Np	-	66.153	89.98	-	66.743	54.654
	Np/Nt	-	0.918	0.818	-	0.9534	0.9937

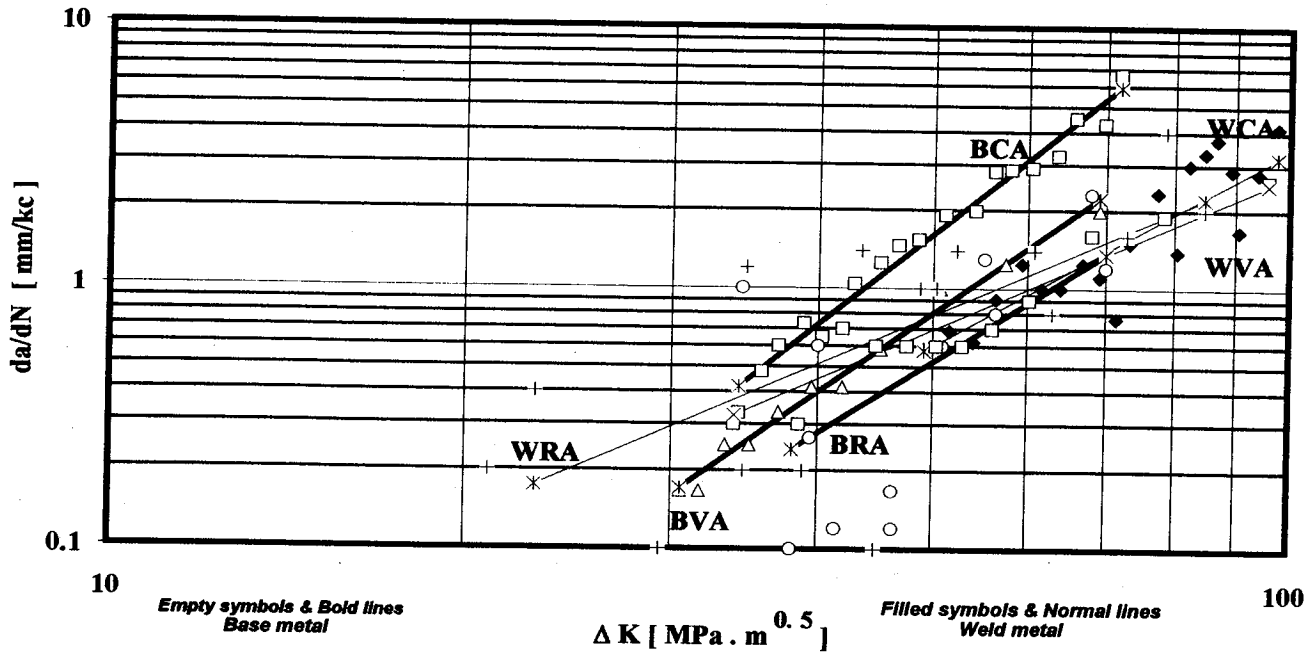

Figure 4. Fatigue crack growth rate (da/dN) vs. stress intensity factor range ΔK.

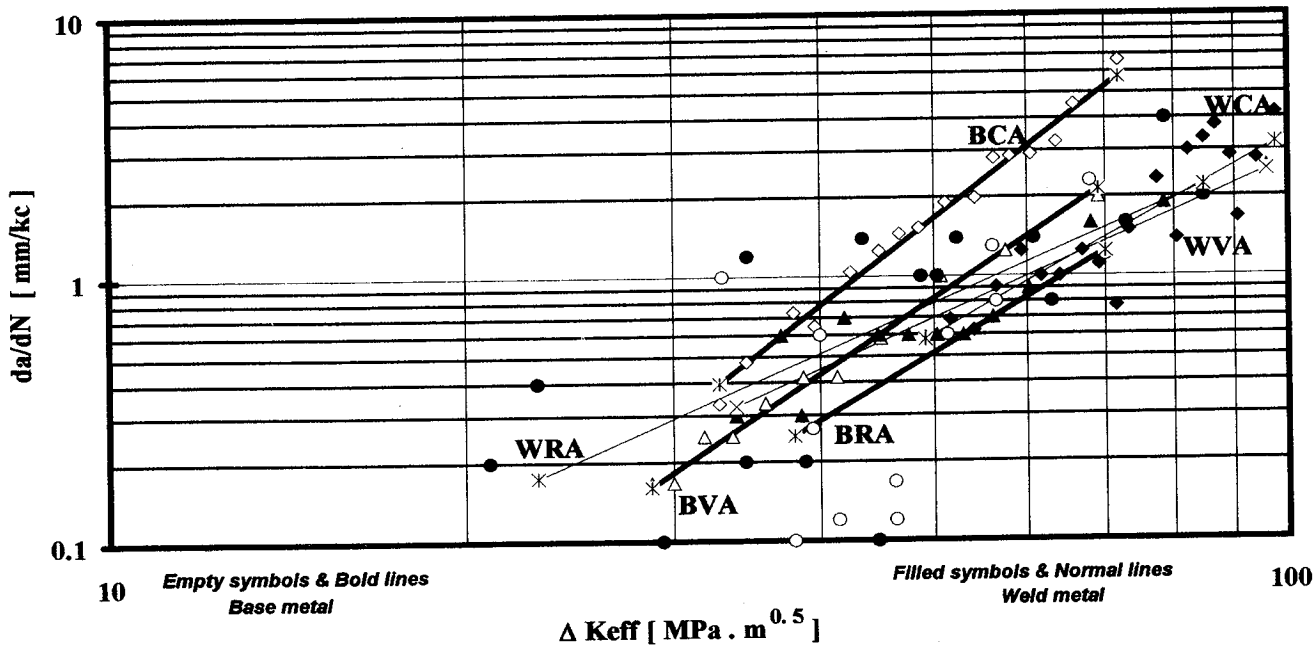

Figure 5. Fatigue crack growth rate (da/dN) vs. effective stress intensity factor range ΔKeff.

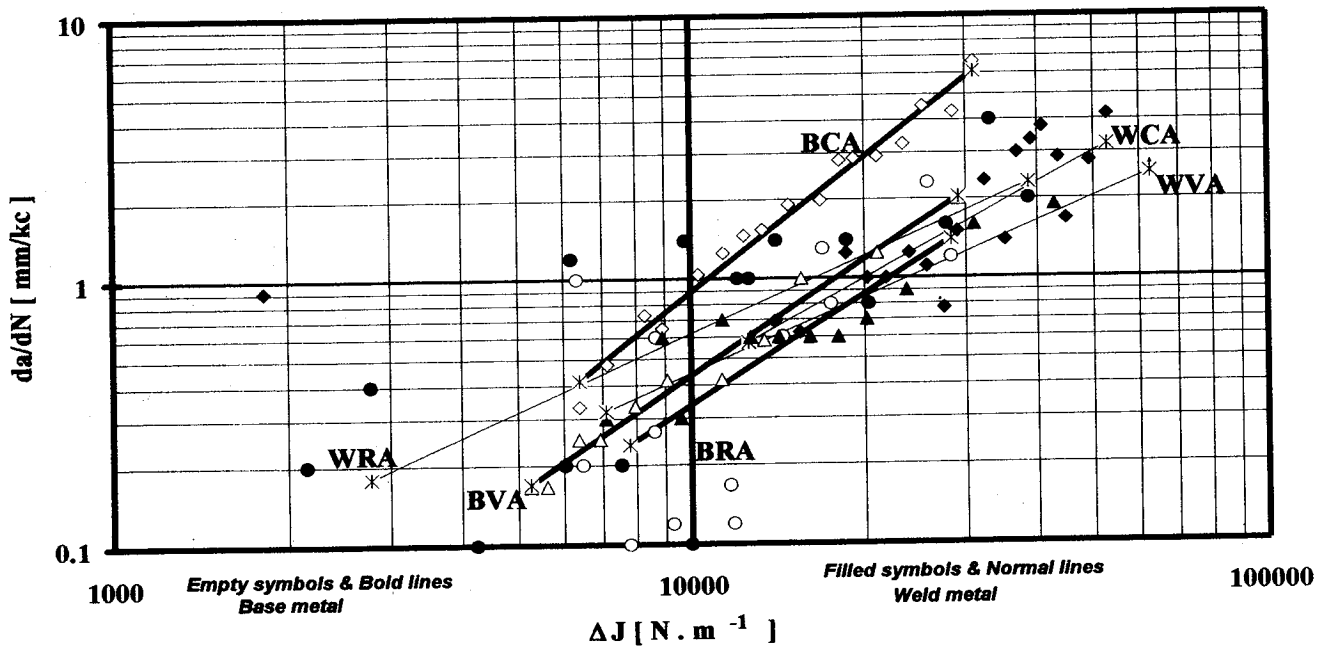

Figure 6. Fatigue crack growth rate (da/dN) vs. cyclic ΔJ-integral.

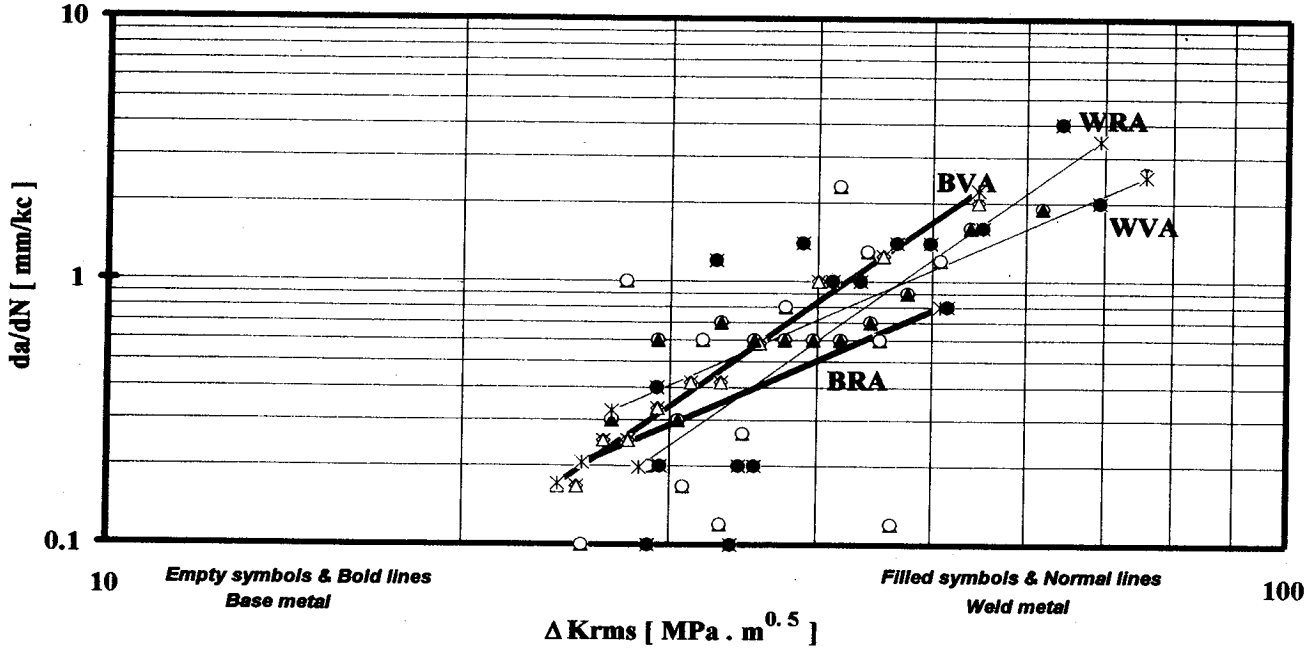

Figure 7 Fatigue crack growth rate (da/dN) vs. root mean square value of the stress intensity factor Krms.

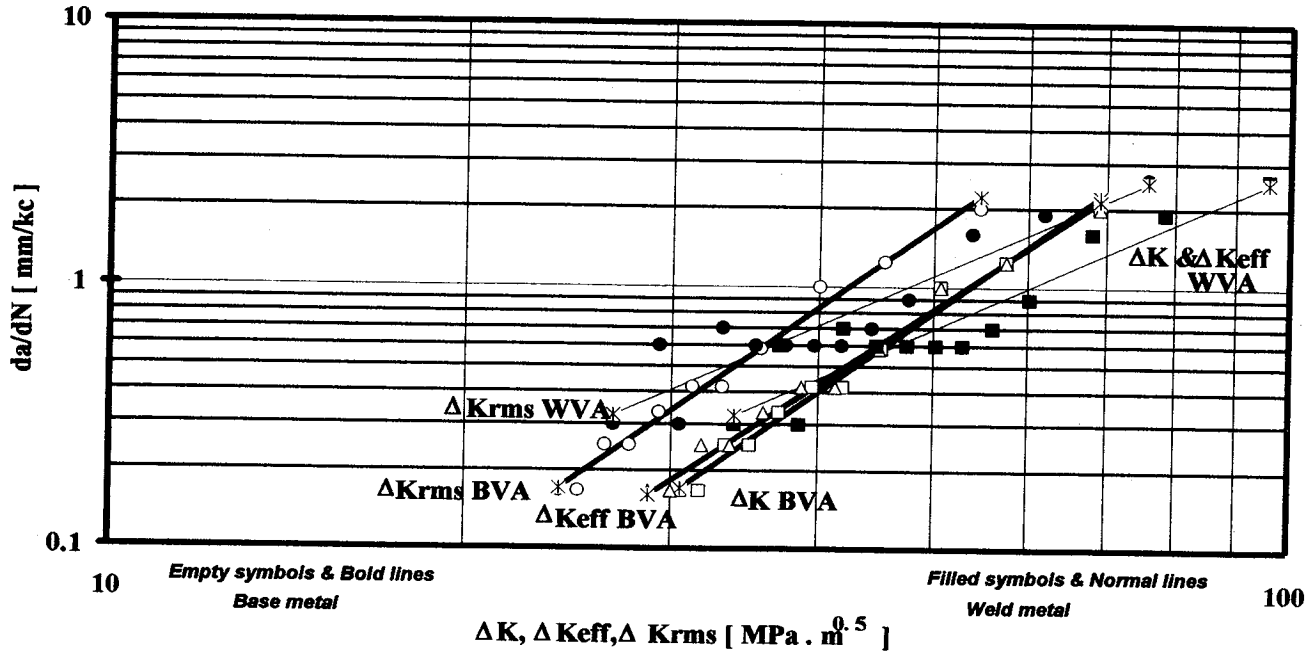

Figure 8. Fatigue crack growth rate (da/dN) vs. ΔK, ΔKeff, ΔKrms of BVA specimen.

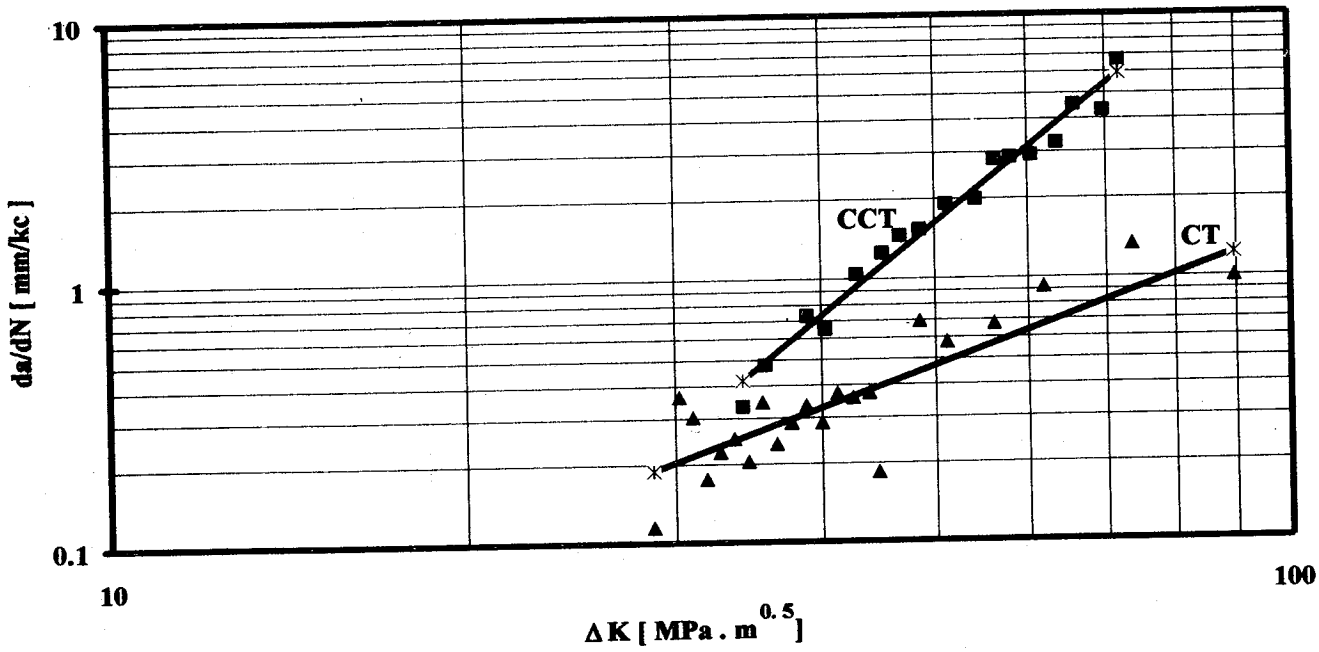

Figure 9. Fatigue crack growth rate (da/dN) vs. ΔK of a CCT and a CT specimen.

b) Residual Stresses

The effect of residual stresses resulting from welding is significant. Data are widely scattered around the lines representing the specimens as shown in figures 4-6 in the case of the weld metal. This influence is not stable, but it varies as the crack grows through the weld metal and through the heat affected zone as well. This is caused by the redistribution of the residual stresses. There is a point of intersection where the crack growth rate of both the base and weld metals coincide in either the growth rate region above or near 0.01 mm/kc.

c) The Loading Sequence

Figure 7 shows the growth rate vs the ΔKrms values of the stress intensity factor of the specimens subjected to variable and random loading amplitudes. This method of crack growth evaluation eliminates the effect of the load sequence. As it can be seen in table 3, comparing K and Krms values of the BVA and the WVA specimens, m was found to be identical in both cases, but C shifted the lines to the region of higher growth rates as also illustrated in figure 8. This is important when considering safety factor calculations in the design of steel constructions subjected to variable amplitude loading. The crack growth rates in this case are doubled related to the type of loading.

d) Fatigue Life Prediction

Table 3 contains the tested and the predicted lives of all specimens as well. Within acceptable accuracy, it was found that, after calculating the fatigue lives, all evaluation concepts fitted with the measured results. This indicates the importance of the results in safe design.

e) CCT and CT Test Specimens

According to the laws of fracture mechanics the results of the CCT and CT test specimens should coincide. By plotting the da/dN vs. ΔK as shown in figure 9, the CT specimen gave lower growth rates . Knowing that the two specimens were tested under the same laboratory conditions , and taking into consideration the reliability of the test results, the CTT specimens may be considered more suitable when testing the fatigue crack growth.

Conclusions

The following conclusions were obtained:

a) The Paris-Erdogan's fatigue crack growth law proved to be a suitable tool for life prediction and is capable of representing the phenomenon under variable amplitude loadings.

b) All the above mentioned evaluation methods provided good life predictions in most of the loading cases. Even the simple ΔK evaluation concept gave good and reliable results.

c) Addition of small loadings decreased the fatigue crack growth rate and thus extended fatigue lives. This is a significant result for both the designer and the maintenance engineer.

d) A confrontation between CT and CCT base metal constant amplitude loading specimens was designed. Results showed lower crack growth rates for CT test specimens in most cases.

e) Fractographical analysis showed no micromorphological difference between surfaces subjected to constant and variable amplitude loading.

f) The effect of the residual stresses on the fatigue crack growth has shown, once more, to be significant in comparing the base metal and welded metal of the same material.

g) Fatigue life prediction results proved to be in good correlation with the experimentally tested and in general they matched well with most of the predicted results found in many modern sources and in some cases seem to be more reliable.

Application of Results

The results of the experiments conducted in this work contribute to a wide range of theoretical and practical applications.

Within the theoretical and methodical framework, modern fracture mechanical concepts were used in the evaluation of results. The findings of the experiments of the fatigue crack growth rate under constant and variable amplitude loading showed that:

a) The CCT type of the test specimens better represent real conditions of constructions with cracks than CT test specimens.

b) The Paris-Erdogan's law is applicable to fatigue life predictions for welded and unwelded components with cracks.

c) The four life prediction methods:ΔK, ΔJ, ΔK_{eff} and ΔK_{rms} can be used with good results including the simple ΔK concept .

The practical contribution of this work can be summarized as follows:

a) The designer and the maintenance engineer are provided with better information about the crack growth in the case of both the base and welded metal under constant and variable amplitude loadings.

b) Tensile overloading caused the retardation of the fatigue crack growth. This can be used not only for checking on the construction's reliability but also for increasing its fatigue life; resulting in enormous economic savings.

c) It is practically advantageous to use the ΔK parameter in the evaluation of fatigue lives of constructions subjected to variable amplitude loadings.

References

1. Ortiz, K.: Stochastic modeling of fatigue crack growth. Engineering Fracture mechanics, 29, 3, 1988, pp.317-334.

2. Ono, H.- Tsunenari, T.: A fatigue crack propagation model for application to service loads. Fatigue Fracture Engineering Materials and Structures,10, 6, 1987, pp.447-460.

3. Dolinski, K.: Fatigue crack growth with retardation under stationary stochastic loading. Engineering Fracture mechanics, 27, 3, 1987, pp.279-290.

4. Rolfe, ST.- Barsom, J.M.: Fatigue crack propagation under variable amplitude load fluctuation. Fracture and fatigue control in structures. Prentice- Hall 1977, pp.268-291.

5. Chang, J.B.- Hudson, C.M.: Methods and models for predicting fatigue crack growth under random loading. ASTM, STP 748, 1981.

6. Katcher, M.: Crack growth retardation under aircraft spectrum loads. Engineering Fracture mechanics, 5, 1973, pp.793-818.

7. Druce, S.G.- Beevers, C.J.- Walker, E.F.: Fatigue crack growth retardation following load reduction in a plain C-Mn steel. Engineering Fracture mechanics, 11, 1979, pp.385-395.

8. Fleck, N.A.: Fatigue crack growth due to periodic underloads and overloads. Acta Metall, 33, 7, 1985, pp.1339-1354.

9. Sunder, R.: A mathematical model of fatigue crack propagation under variable amplitude loading. Engineering Fracture mechanics, 12, 1979, pp.155.-165.

10. Arone, R.: Fatigue crack growth under random overloads superimposed on constant amplitude cyclic loading. Engineering Fracture mechanics, 24, 2, 1986, pp.223-232.

11. Ulrich, K.: Fatigue crack growth in welded joints. Ph.D. dissertation. Bratislava 1980.

12. Blodgett, O.W.: Designing weldments for fatigue loading. Welding Journal, 71, 7,, 1992, pp.39-44.

13. Lim, J.K.- Stephens, R.I.: Fatigue crack growth and retardation in the welded HAZ of 4140 steel. Welding Journal, 69, 8, 1990, pp. 294s- 304s.

14. Sidawi, J.A.: Fatigue crack growth under variable amplitude loading. Ph.D. dissertation. Slovak Academy of Sciences & Welding Research Institute, Bratislava, Slovakia, 1989.

15. Paris, P.C.: The fracture mechanics approach to fatigue. An interdisciplinary approach. Syracuse university press, 1964, pp.107-127.

16. Skroupa, M.: Fatigue life prediction of cruciform joints failing at the weld toe. Welding Journal, 71, 8, 1992, pp.269s- 275s.

17. Sobczyk, K.: Modeling of random fatigue crack growth. Engineering Fracture mechanics, 24, 4, 1986, pp.609-623.

18. IIW recommendation: The application of an engineering critical assessment in design, fabrication and inspection to assess the fitness for purpose welded products. Part 4, Fatigue. Com. V-878-88, X-1167-88, XIII-1283-88, XV-665-88, 03-06-1988.

19. Gregor, V.- Sidawi, J.A.: Calculation of the damage cumulation in welded beams. Welding News, Welding Research Institute, Bratislava, Slovakia, 1, 40, 1990, pp.1-8.

20. Gregor, V.- Ulrich, K.- Sidawi, J.A.: Fatigue life of welded I beams under bending loads of 15422.5 & 11523.1 steels. Welding Research Institute, Bratislava, Slovakia, 1584/3/205, 1984.

21. ASTM Standard E 647-93: Standard test method for measurement of fatigue crack growth rates. Annual Book of Standards, Vol.03.01, 1993, pp. 679-706.

22. Dowling, N.E.: J-integral estimates for cracks in infinite bodies. Engineering Fracture mechanics, 26, 3, 1987, pp.333-348.